Hybrid Plasmonic & Semiconductor Nanostructures for Quantum-Photon and Coherent Multi-Photon Generation and Control

Andrei Piryatinski

Theoretical Division
Los Alamos National Laboratory

Virtual International Seminar on Theoretical Advancements (VISTA)

January 15, 2025

LA-UR-25-20319

Outline:

- ✓ Introduction: Surface-plasmon resonances & Purcell effect
- ✓ Surface-plasmon Purcell enhancement of quantum dot emission in near-IR telecom spectral bands
- ✓ Nonlinear lasing/light amplification in quantum dot arrays interacting with Ag-nanopillar lattices
- ✓ Parametric Amplification & Spontaneous parametric downconversion (PDC) in arrays of Au-metal nanoparticles
- ✓ Summary & outlook

Introduction: surface plasmon resonances & Purcell effect

- In metals according to Drude response model electron gas plasma resonance frequency (UV) depends on electron concentration

$$\omega_{\mathrm{p}} = \sqrt{\frac{n q_{\mathrm{e}}}{m_{\mathrm{e}} \epsilon_0}}$$

- For surface plasmons geometry /nano- structuring allows to tune the resonance frequency within visible spectral range

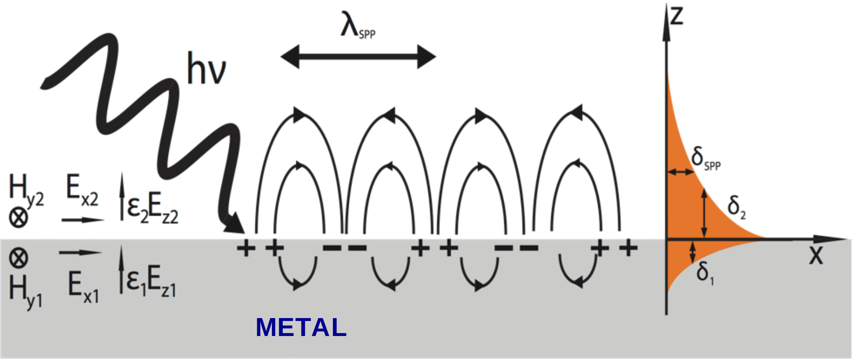

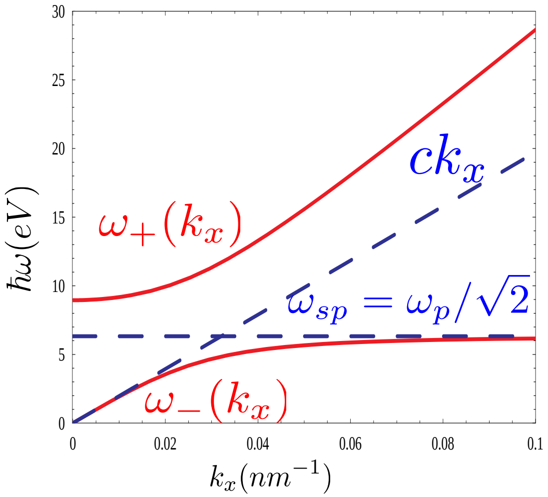

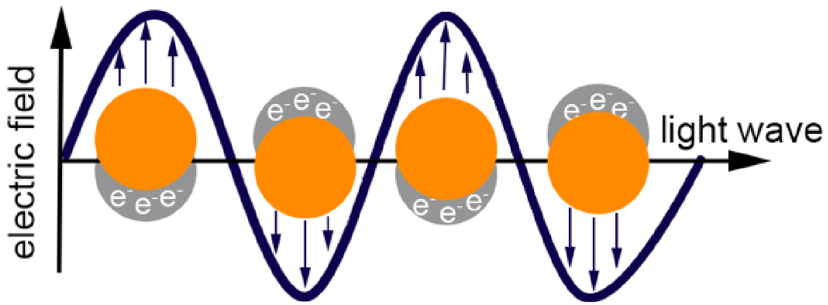

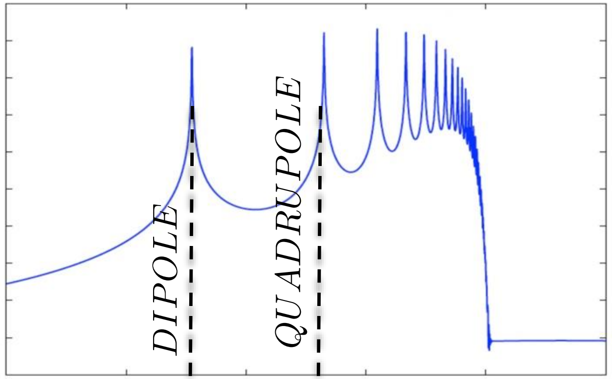

Purcell effect: enhancement of spontaneous decay for a quantum emitter (quantum dot, molecule, etc.) in the vicinity of metal nanoparticle

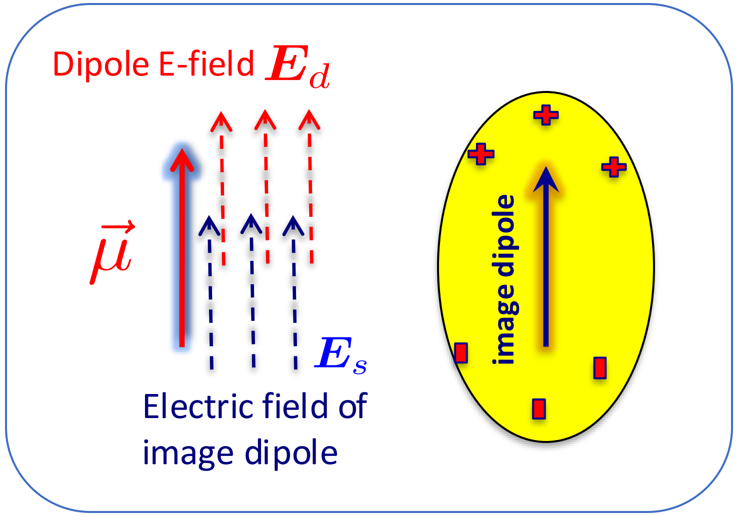

Classical interpretation: Metal polarization produces image dipole whose field interacts with the transition dipole

Quantum interpretation: enhancement of local photon DOS due to plasmon enhanced electromagnetic field density of state

Spinel metal oxide: Fe_3O_4 nanocrystals (NCs) as building blocks for near-IR telecom band plasmonics

Most of surface plasmon resonances of noble metal nanoparticles and nanoparticle arrays cover visible spectral range. It is desirable to achieve plasmonic response in the near-IR, i.e., telecom band, for optoelectronic applications, including room-T single photon sources.

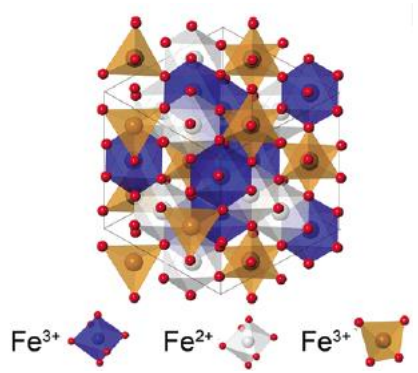

- Fe_3O_4 NC represent degenerate (self-doping) semiconductor materials
- Ratio of Fe^{2+}:Fe^{3+} cations determines concentration of free electrons forming plasmonic response in the near-IR

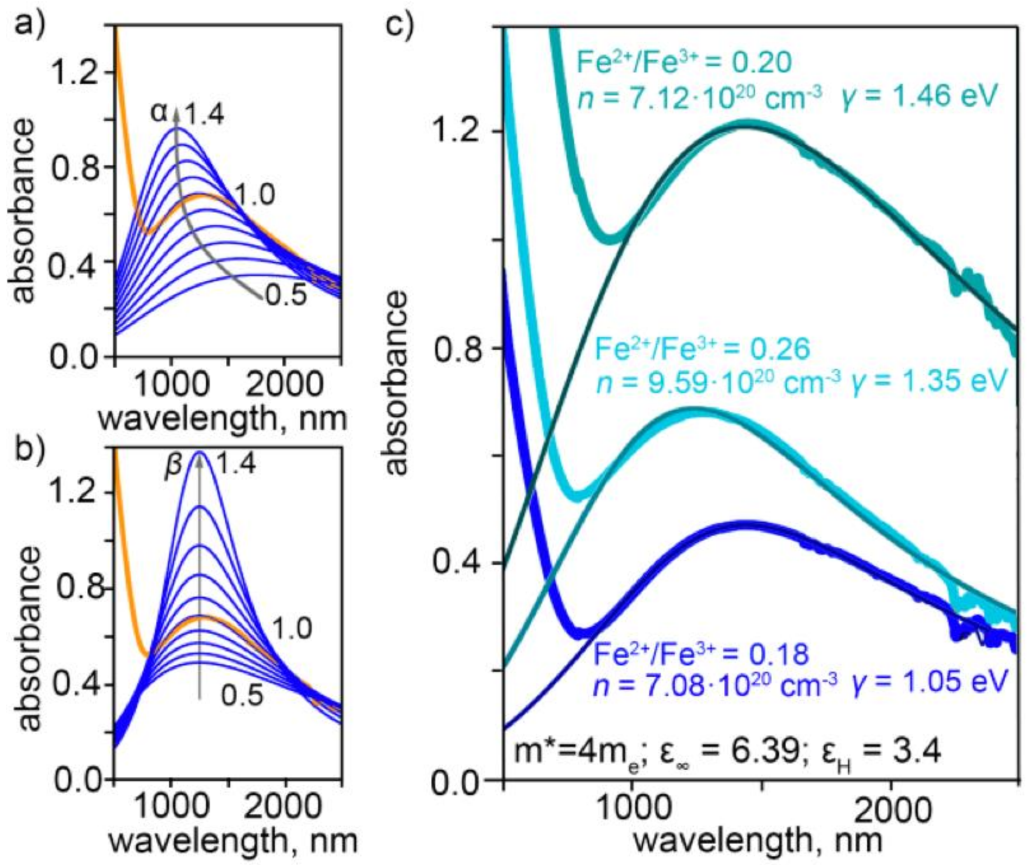

- Fitting the light scattering spectra of Fe_3O_4 NC using Mie model along with the Drude model we extracted the electron densities for various Fe^{2+}:Fe^{3+} ratios corresponding to the size-dependent near-IR plasmonic response as well as the dissipation rates

E. Dologopolova, *et al. Nanoscale Horizons*, **7** 267 (2022).

Simulated and measured Purcell enhancement rates for array of PbS/CdS QDs on top of Fe_3O_4 NCs

- Purcell enhancement factor is the ratio γ_t/γ_t^0 of the total (radiative + nonradiative) decay rate of exciton states in QDs in the presence of Fe_3O_4 NCs, γ_t to the total decay rate in the absence of Fe_3O_4 NCs, γ_t^0

- Plasmonic nanoparticles form low-Q cavity and some of the energy transferred from QDs to array of Fe_3O_4 NCs gets dissipated via Ohmic losses to heat

- For the light emitting application purpose we need to know the radiative Purcell factor γ_r/γ_r^0, where γ_r is the radiative decay rate of QDs in the presence of Fe_3O_4 NCs and γ_r^0 is the radiative decay rate of QDs in the absence of Fe_3O_4 NCs.

-Experimental spectra: Absorption of Fe_3O_4 NCs & PL of PbS/CdS QDs

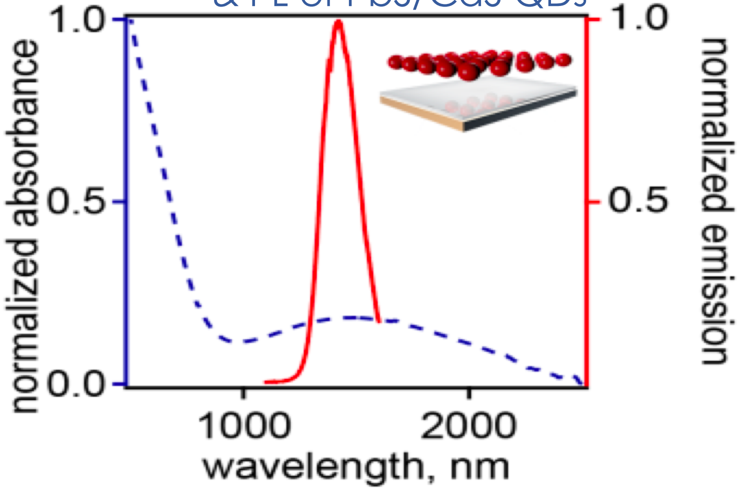

- Modeling total Purcell factor for different spacers

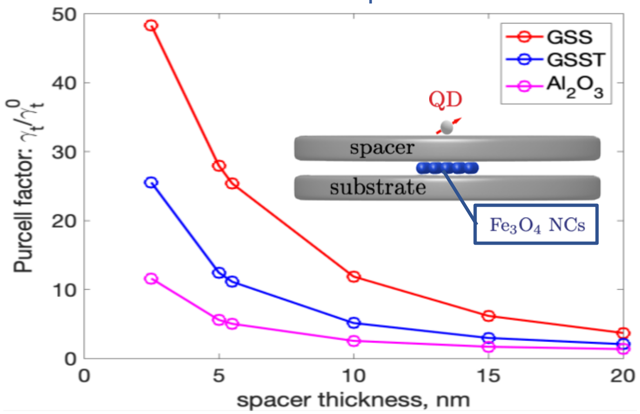

-Experiment: Purcell factor (PL decay rate with and without Fe_3O_4 NC layer for various spaces

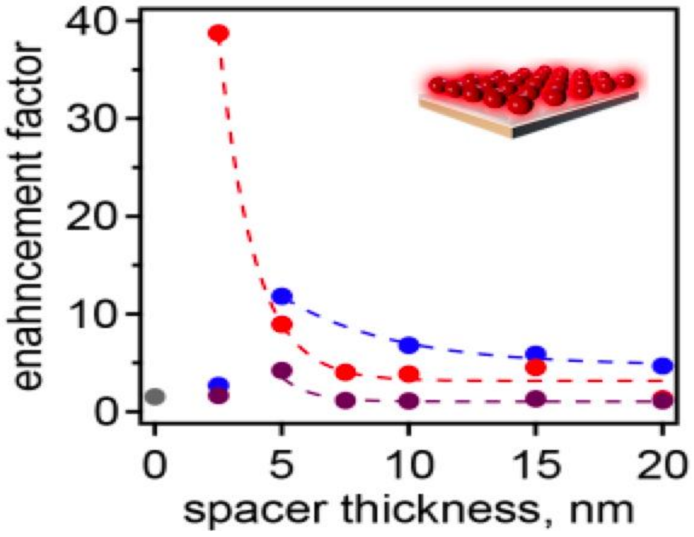

- Modeling radiative Purcell factor for different spacers

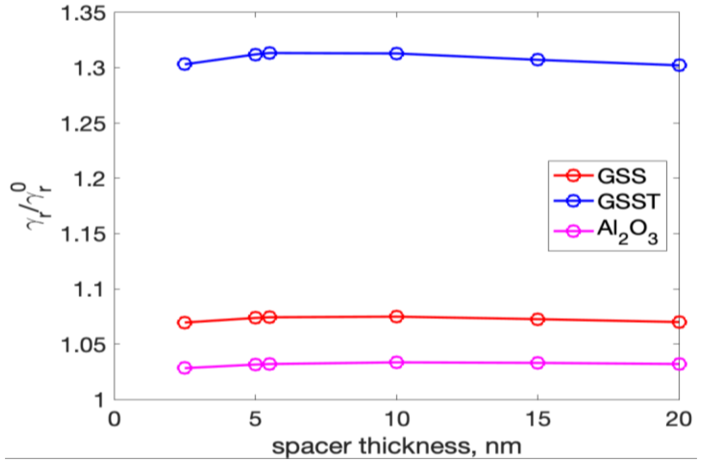

Most of the emitted energy is dissipated to heat, radiative factor is low requiring improved design of plasmonic cavity

E. Dologopolova, *et al. Nanoscale Horizons*, **7** 267 (2022).

Purcell enhancement of quantum dot emission rate using Fe_3O_4 patch antenna

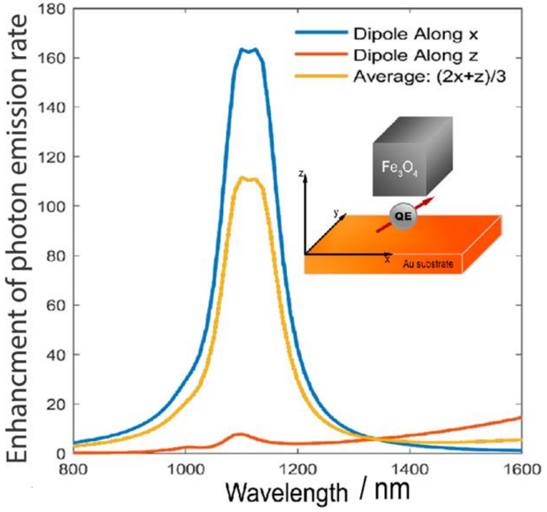

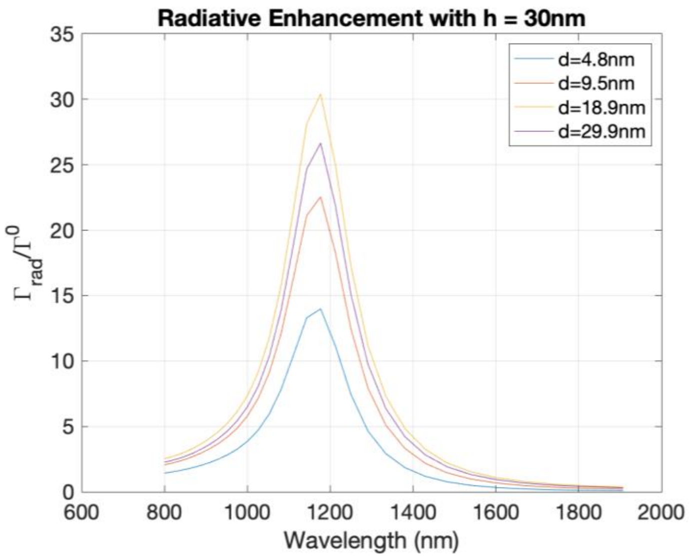

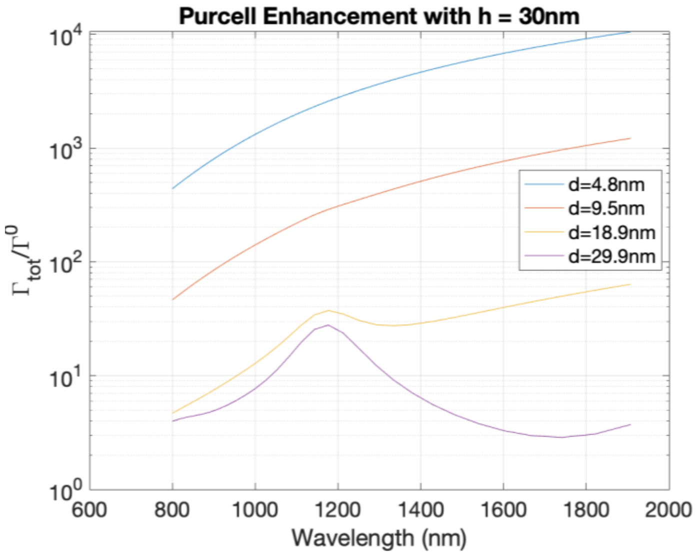

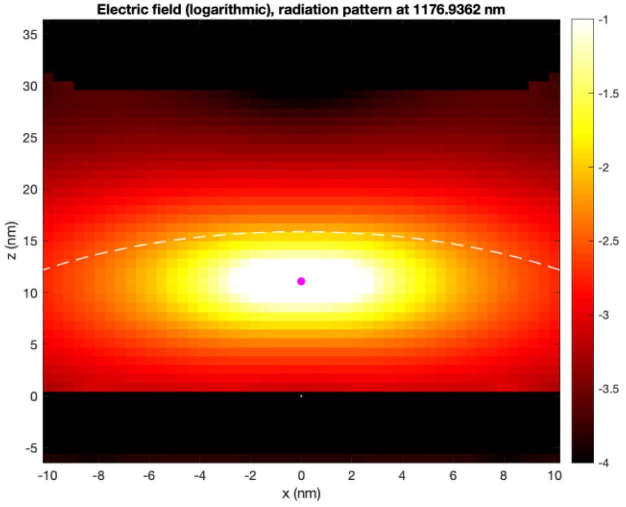

- The radiative enhancement is low when close to the cube and is maximized when closer to the substrate.
- As the QD moves away from the cube, the nonradiative decay rate quickly decreases. Just above the substrate, most of the total decay rate is radiative in nature.
- Experimental validation is pending

Quantum & nonlinear plasmonics in <u>strong coupling regime</u>

Quantum plasmonics:

- Purcell effect (plasmon-enhanced spontaneous emission)
- Lasing & superradiance

Nonlinear optics of plasmonic nanostructures:

- Optical bistabilities
- Harmonics generation
- Four-wave mixing

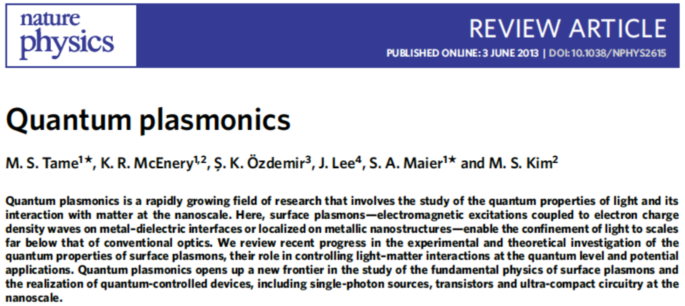

nature physics | REVIEW ARTICLE
PUBLISHED ONLINE: 3 JUNE 2013 | DOI: 10.1038/NPHYS2615

Quantum plasmonics

M. S. Tame[1]*, K. R. McEnery[1,2], Ş. K. Özdemir[3], J. Lee[4], S. A. Maier[1]* and M. S. Kim[2]

Quantum plasmonics is a rapidly growing field of research that involves the study of the quantum properties of light and its interaction with matter at the nanoscale. Here, surface plasmons—electromagnetic excitations coupled to electron charge density waves on metal–dielectric interfaces or localized on metallic nanostructures—enable the confinement of light to scales far below that of conventional optics. We review recent progress in the experimental and theoretical investigation of the quantum properties of surface plasmons, their role in controlling light–matter interactions at the quantum level and potential applications. Quantum plasmonics opens up a new frontier in the study of the fundamental physics of surface plasmons and the realization of quantum-controlled devices, including single-photon sources, transistors and ultra-compact circuitry at the nanoscale.

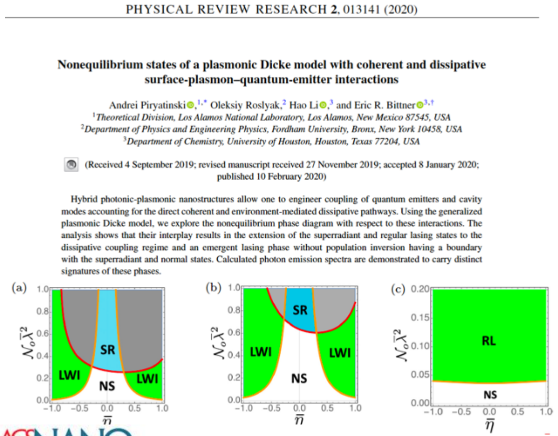

PHYSICAL REVIEW RESEARCH **2**, 013141 (2020)

Nonequilibrium states of a plasmonic Dicke model with coherent and dissipative surface-plasmon–quantum-emitter interactions

Andrei Piryatinski[1,*], Oleksiy Roslyak[2], Hao Li[3] and Eric R. Bittner[3,†]
[1]Theoretical Division, Los Alamos National Laboratory, Los Alamos, New Mexico 87545, USA
[2]Department of Physics and Engineering Physics, Fordham University, Bronx, New York 10458, USA
[3]Department of Chemistry, University of Houston, Houston, Texas 77204, USA

(Received 4 September 2019; revised manuscript received 27 November 2019; accepted 8 January 2020; published 10 February 2020)

Hybrid photonic-plasmonic nanostructures allow one to engineer coupling of quantum emitters and cavity modes accounting for the direct coherent and environment-mediated dissipative pathways. Using the generalized plasmonic Dicke model, we explore the nonequilibrium phase diagram with respect to these interactions. The analysis shows that their interplay results in the extension of the superradiant and regular lasing states to the dissipative coupling regime and an emergent lasing phase without population inversion having a boundary with the superradiant and normal states. Calculated photon emission spectra are demonstrated to carry distinct signatures of these phases.

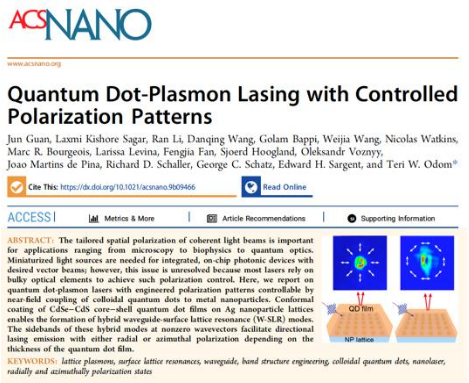

ACS NANO

Quantum Dot-Plasmon Lasing with Controlled Polarization Patterns

Jun Guan, Laxmi Kishore Sagar, Ran Li, Danqing Wang, Golam Bappi, Weijia Wang, Nicolas Watkins, Marc R. Bourgeois, Larissa Levina, Fengjia Fan, Sjoerd Hoogland, Oleksandr Voznyy, Joao Martins de Pina, Richard D. Schaller, George C. Schatz, Edward H. Sargent, and Teri W. Odom*

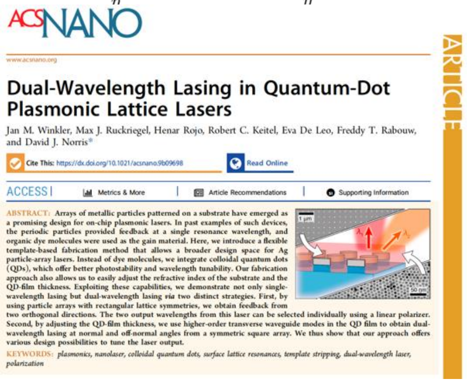

ACS NANO

Dual-Wavelength Lasing in Quantum-Dot Plasmonic Lattice Lasers

Jan M. Winkler, Max J. Ruckriegel, Henar Rojo, Robert C. Keitel, Eva De Leo, Freddy T. Rabouw, and David J. Norris*

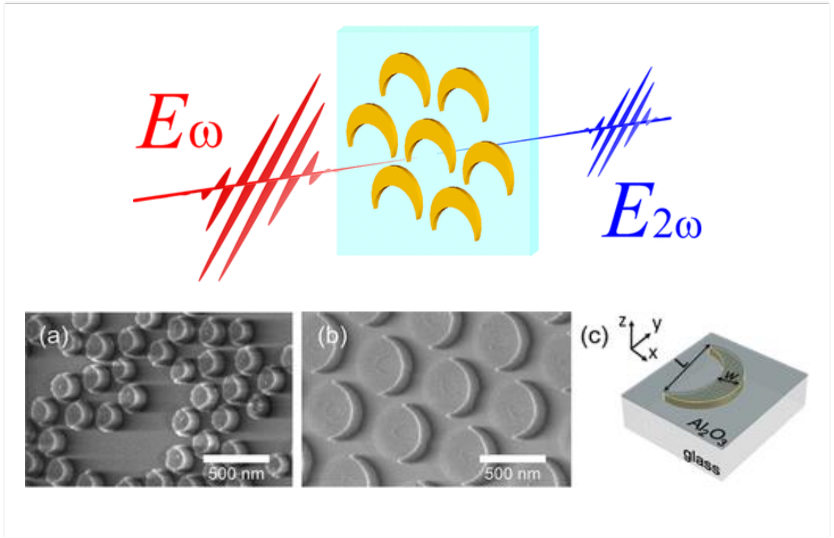

H. Maekawa, et. al., Wavelength and polarization dependence of second-harmonic responses from gold nanocrescent arrays, J. Phys. Chem. C 124, 20424 (2020).

- We introduce nonlinear plasmonoic cavity & examine the effect of QEs on SHG/PDC;
- Use both: quantum optics & semiclassical plasmonic models

Driven-dissipative dynamics in $\chi^{(2)}$-nonlinear plasmonic cavity: Second-harmonic generation (SHG) and QD gain effect

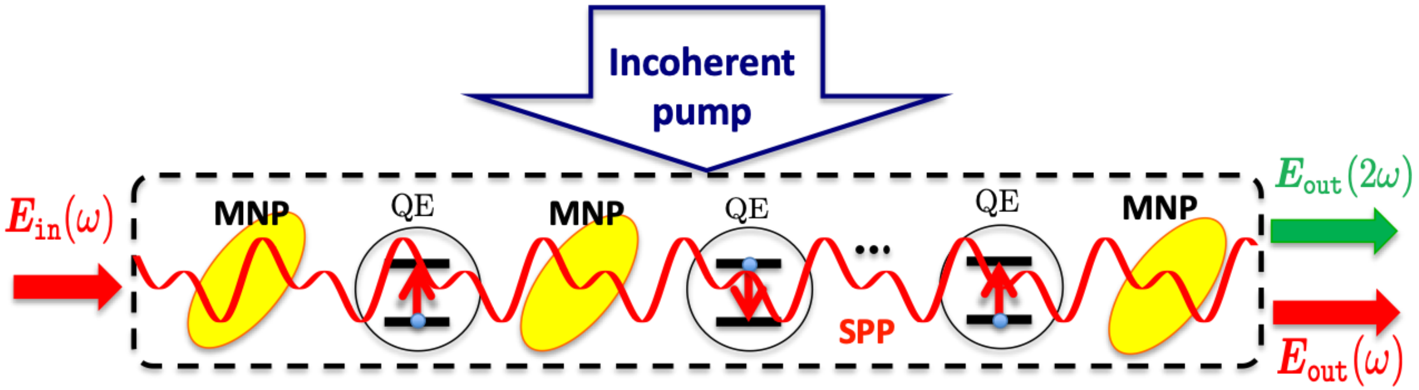

- Array of metal nanoparticles (MNPs) forms a collective mode named the Surface Lattice Resonance (SLR)
- Compared to Local Surface Plasmon Resonances (LSPR) of each MNP, the SLR shows narrow lineshape (low losses), i.e., higher-Q cavity mode.

- Ensemble of $\mathcal{N}_o$ quantum emitters (QE)/ quantum dots (QD) or dye molecules interacts at fundamental frequency ω with the SLR cavity mode with coupling rate $\sqrt{\mathcal{N}_o}\lambda$

- Beyond previously considered effects, we introduce the non-linear $\chi^{(2)}$ -response of MNPs.
- Weak probe field $E_{in}(\omega)$ initiates second-harmonic generation, $E_{out}(2\omega)$, associated with combined of SLR and QEs response
- Incoherent pump the QDs above population inversion results in the optical gain whose effect we want to understand on the second harmonic signal $E_{out}(2\omega)$.

M. Sukharev, O. Roslyak, & A. P., J. Chem. Phys. 154, 084703 (2021).

Strong coupling regime: Exciton-plasmon-polaritons

Weak plasmonic anharmonicity

(A) (B) (C)

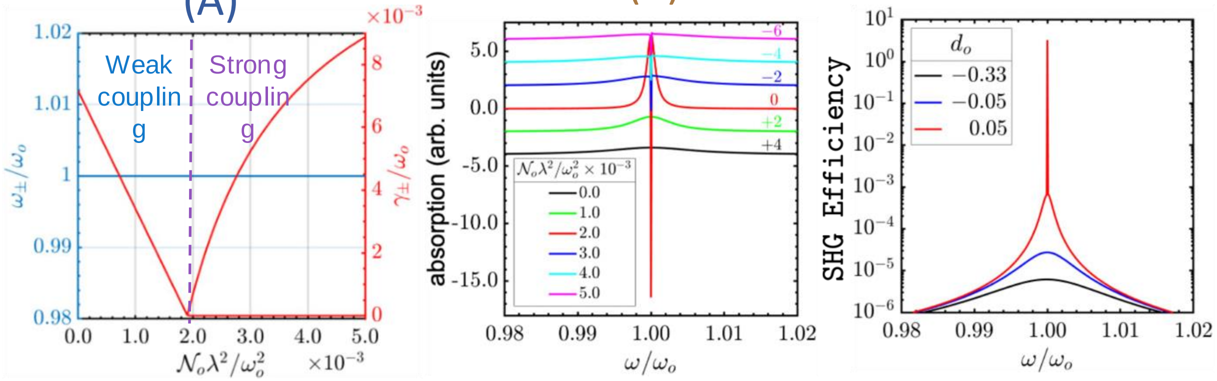

Strong plasmonic anharmonicity

(A) (B) (C)

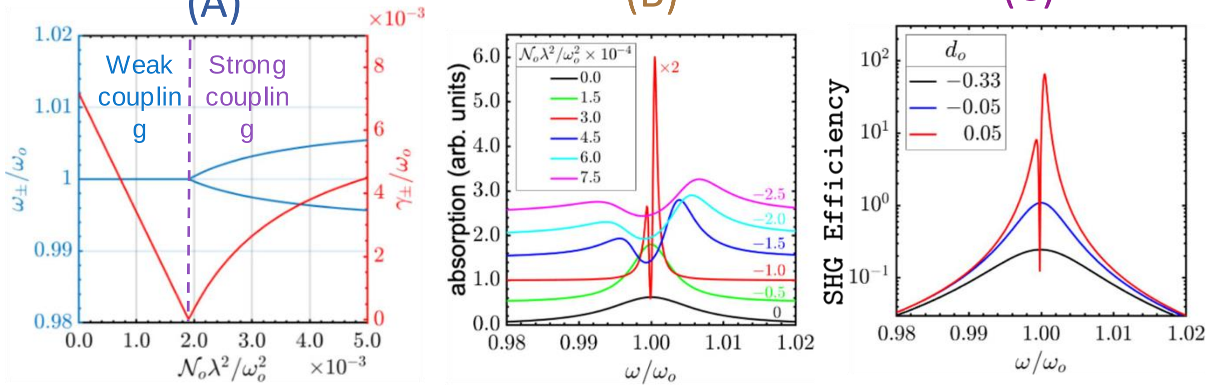

Above critical coupling (strong coupling regime) $\mathcal{N}_o\lambda_c^2 \sim \gamma_{sp}\gamma_o$:

Weak plasmonic anharmonicity:

A. No Rabi splitting observed but QE gain fully compensates losses for low-polariton

B. Lasing transition / Incident field amplification

C. Amplified polariton field converts into SH via $\chi^{(2)}$-nonlinear process resulting in SHG efficiency enhancement $\sim 10^5$

Strong plasmonic anharmonicity:

A. Rabi splitting observed but QE gain partially compensates losses

B. No lasing transition / polariton splitting & narrowing of absorption line

C. Polariton field receives partial amplification by strong anharmonicity enhances $\chi^{(2)}$-nonlinearity boosting SHG efficiency $\sim 10^3$

M. Sukharev, O. Roslyak, & A. P., J. Chem. Phys. 154, 084703 (2021).

Simulations of amplified SHG in Ag-lattice coupled to layer of CdSe QEs

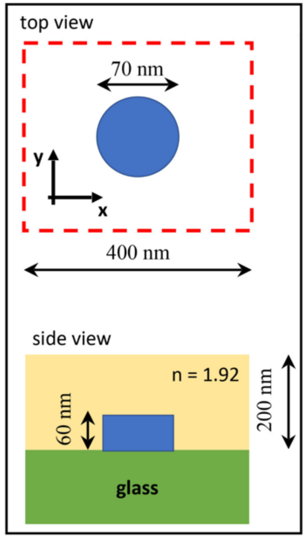

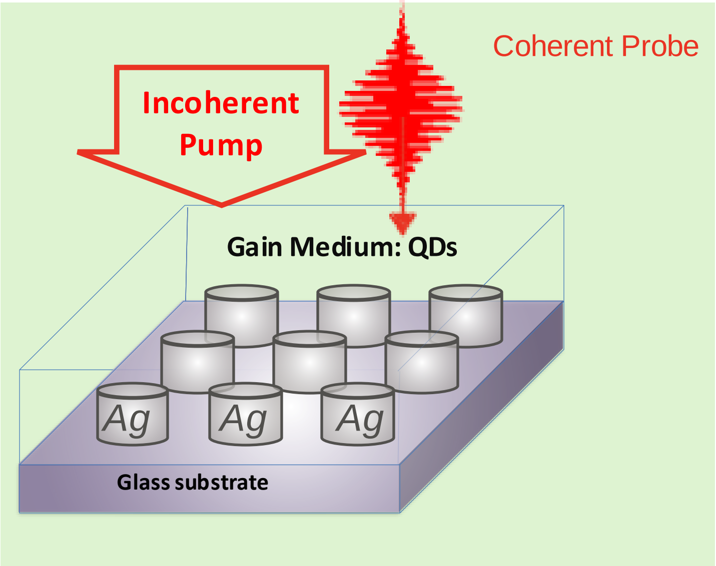

Nano-structure: square lattice of Ag nano-pillars filled with two-level QEs parameterized for CdSe QDs

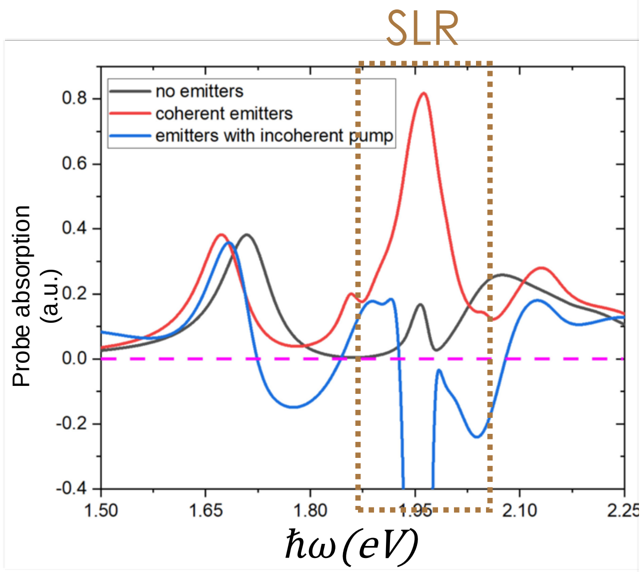

Probe absorption spectrum:

- Surface lattice resonance (SLR) $\hbar\omega \sim 1.95\,eV$

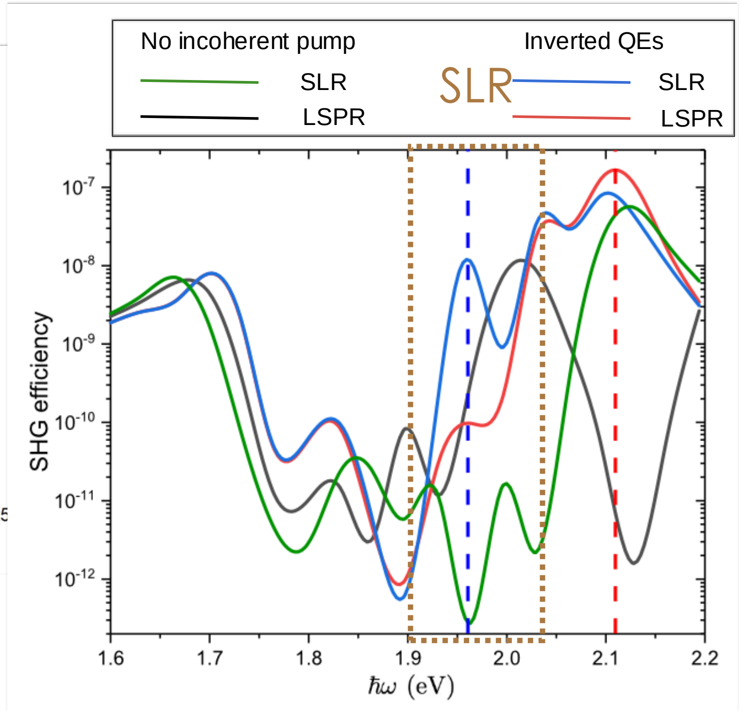

- SHG efficiency enhancement factor @ SLR $\sim 10^5$

- Probe amplification (negative absorption) @ SLR for inverted QEs.

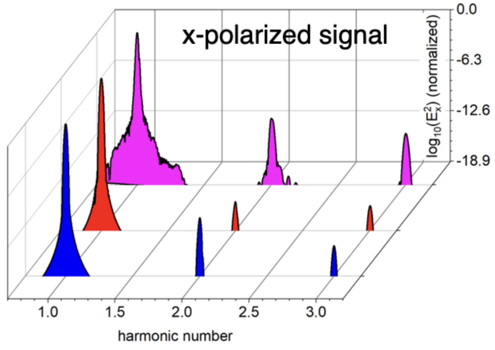

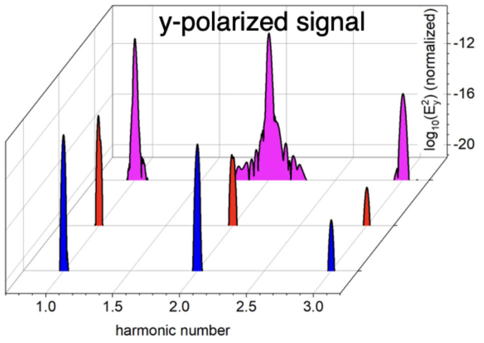

In both panels excitation field is polarized in the x-direction resulting in the enhanced SHG due to $\chi^{(2)}_{yxx}$ (compare magenta curves). Red: QEs are below inversion. Blue: no QEs.

M. Sukharev, O. Roslyak, & A. P., J. Chem. Phys. 154, 084703 (2021).

Simulations of SHG and DFG (THz pulses) for Au MNP possessing C_{2v} symmetry

- Geometry & linear response

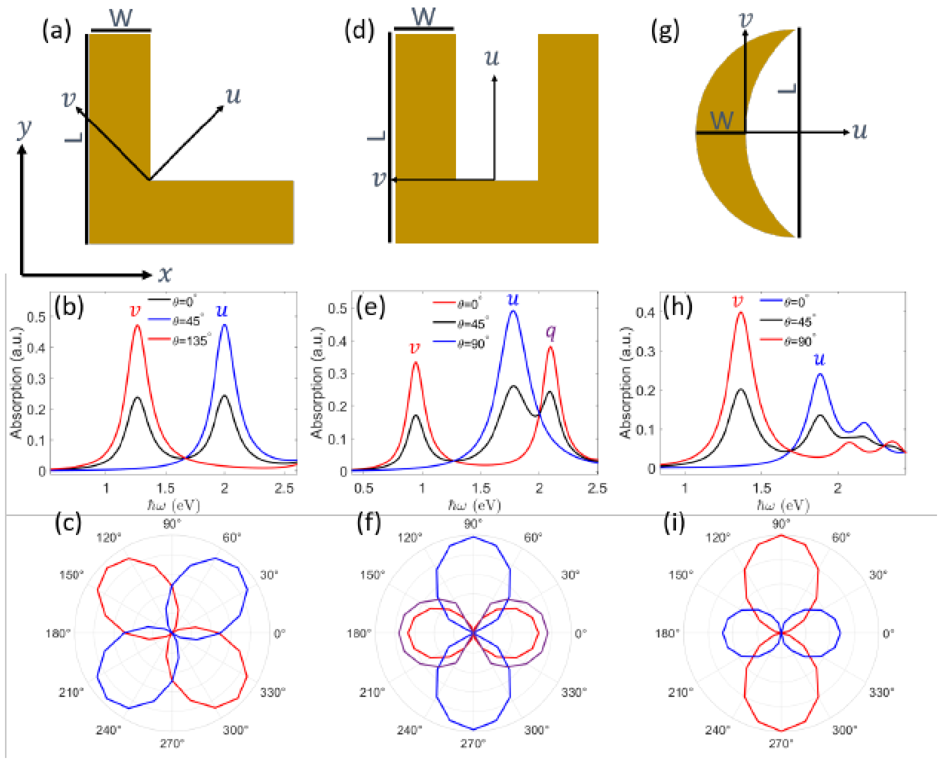

- Normalized SHG intensity along natural (u, v)-axis for C_{2v} MNP as function of pump polarization & energy:

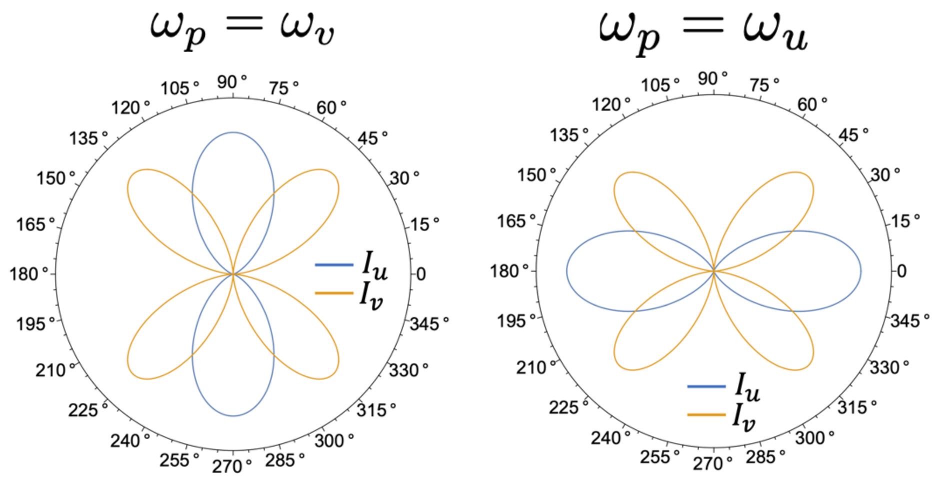

- SHG field depends on the pump field polarization as

$$E_u \sim \chi^{(2)}_{uuu} E_u E_u + \chi^{(2)}_{uvv} E_v E_v$$
$$E_v \sim \chi^{(2)}_{vvu} E_v E_u + \chi^{(2)}_{vuv} E_u E_v$$

- Identifying three independent second-order susceptibility tensor components:

$$\chi^{(2)}_{uuu} \neq \chi^{(2)}_{uvv} \qquad \chi^{(2)}_{vvu} = \chi^{(2)}_{vuv}$$

- Power spectra of nonlinear response:

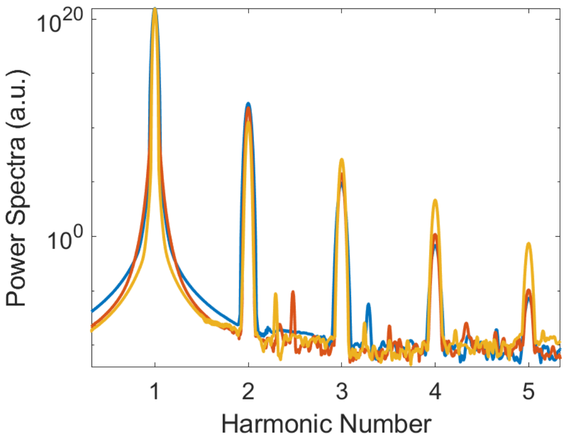

M. R. Clark, S. A. Shah, A. P., M. Sukharev, J. Chem. Phys **161** 104107, (2024).

DFG & parametric amplification in L-shaped Au-nanoparticle array $\Lambda = 400nm$

- Considered array of non-interacting L-shaped MNPs (lattice resonances are not significant compared to local surface plasmon resonances). Treated array as an effective medium, we evaluated parametric gain and identified conditions for the parametric amplification regime

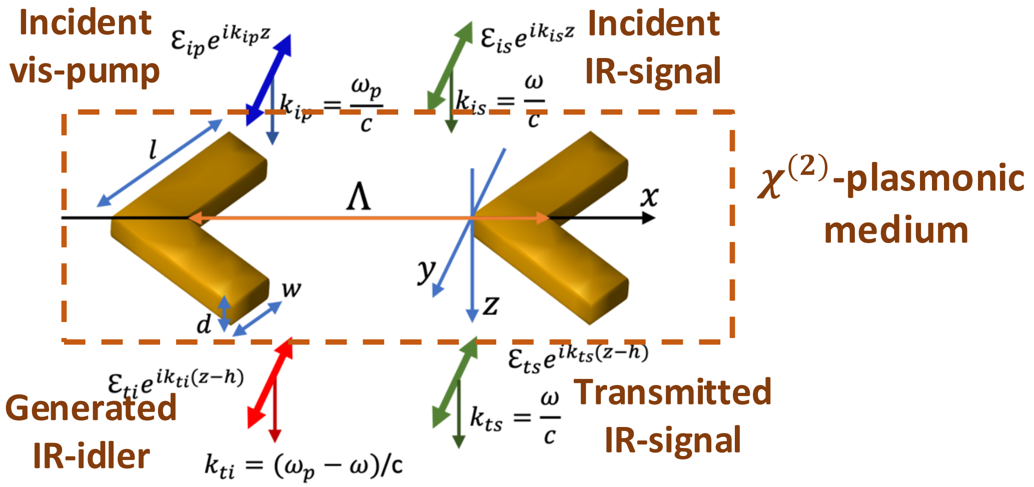

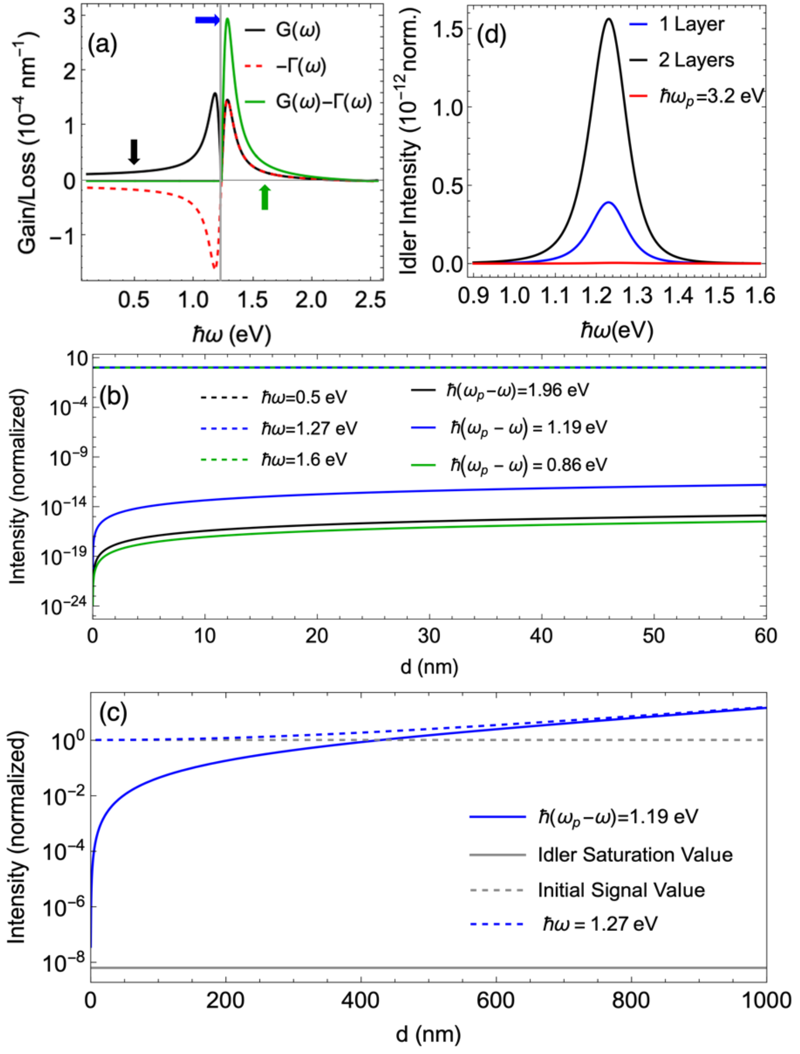

- We have performed simulations of surface-plasmon gain enhanced parametric amplification processes
- The simulations demonstrate that a multi-layered structure d~500nm can support the signal amplification regime
- Evaluations of Spontaneous Parametric Down-Conversion (SPDC) processes in Au-MNP arrays resulting in quantum photon generation require quantum optical simulations

S. Shah, M. R. Clark, J. Zyss, M. Sukharev, A. P., *Opt. Lett.* **49** 1680 (2024).

Modeling of SPDC in C_{2v} Au-nanoparticle array with intrinsic nonlinearity

- Surface plasmon enhanced SPDC process:

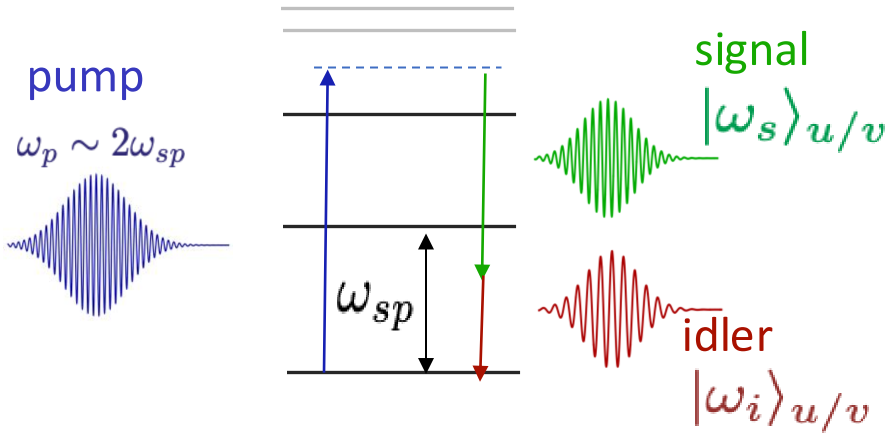

- Two biplasmon/biphoton states can be prepared by the pump, respectively polarized along u and v axes:

$$|\Psi_{2\mathrm{sp}}\rangle_u = \iint d\omega_s d\omega_i \{\mathcal{F}_{uuu}(\omega_s\omega_i)|\omega_s\rangle_u|\omega_i\rangle_u + \mathcal{F}_{uvv}(\omega_s\omega_i)|\omega_s\rangle_v|\omega_i\rangle_v\}$$

$$|\Psi_{2\mathrm{sp}}\rangle_v = \iint d\omega_s d\omega_i \mathcal{F}_{vuv}(\omega_s\omega_i)\{|\omega_s\rangle_u|\omega_i\rangle_v + |\omega_s\rangle_v|\omega_i\rangle_u\}$$

- Central quantity describing the biplasmon/biphoton wavepacket is joint spectral amplitude $\mathcal{F}_{\alpha\beta\gamma}(\omega_s\omega_i)$

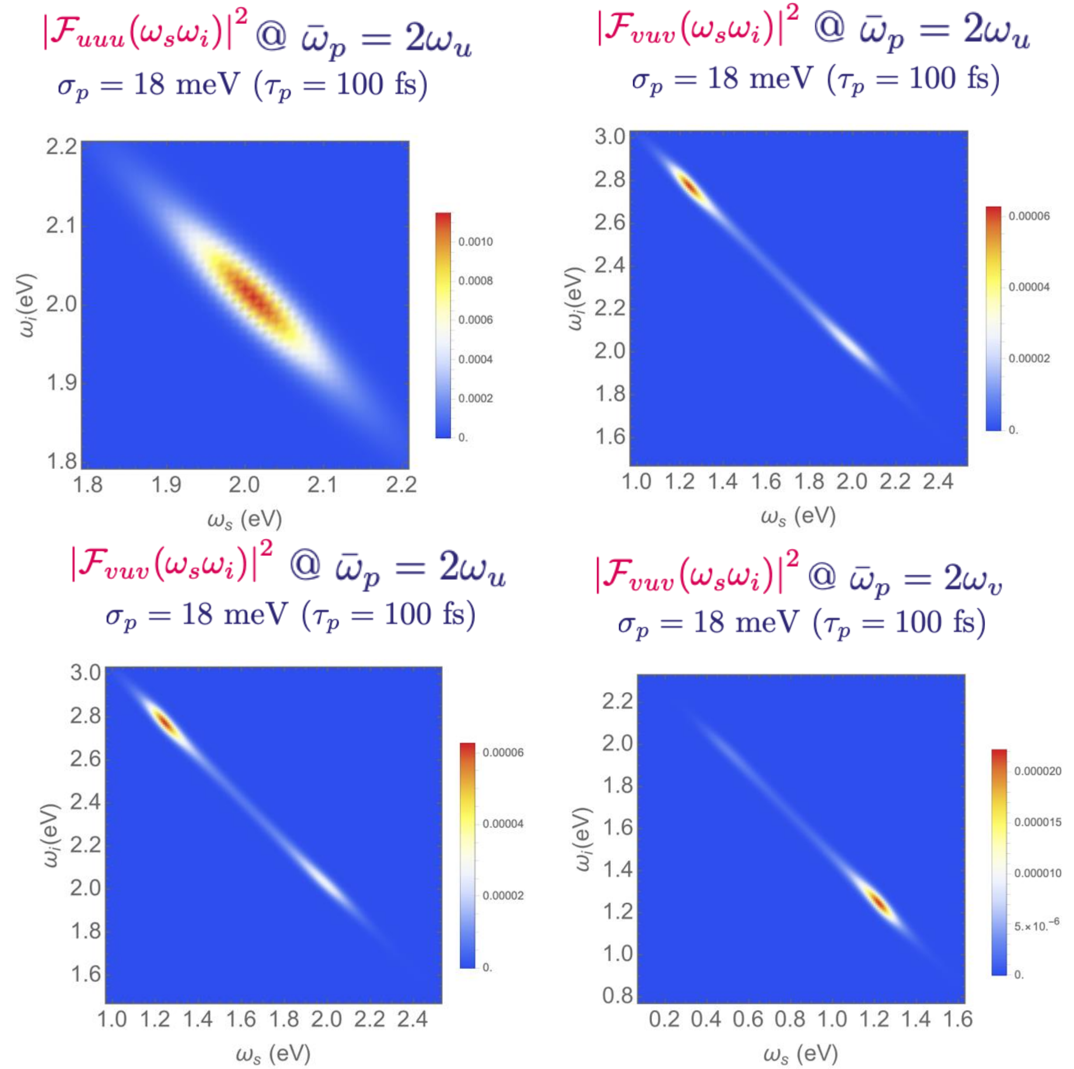

S. A. Shah, M. R. Clark, J. Zyss, M. Sukharev, A. P., (*in preparation*).

Calculation of SPDC Yield for L-shaped Au-nanoparticle array $\Lambda = 400nm$ via

- Besides the parametric amplification processes reported a year ago we considered the SPDC process of creating the signal & idler photons out of vacuum plasmon vacuum fluctuations

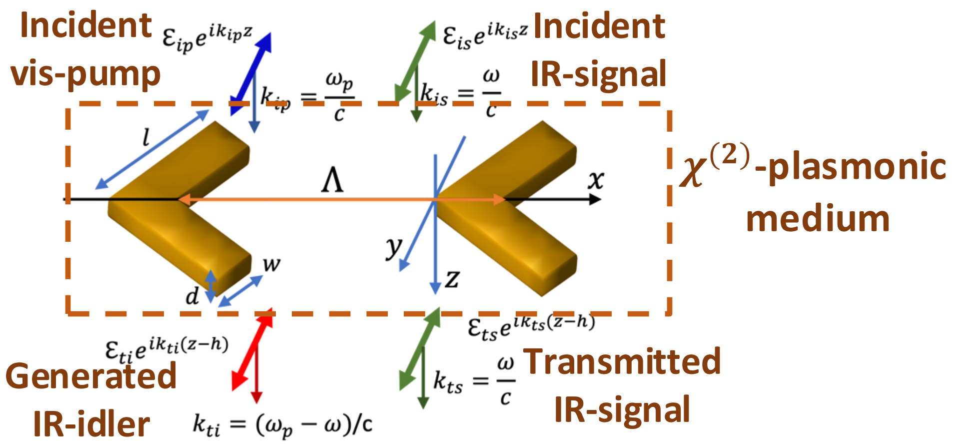

- Level diagram $\chi^{(2)}$-plasmonic response & SPDC process using quantum anharmonic oscillator model

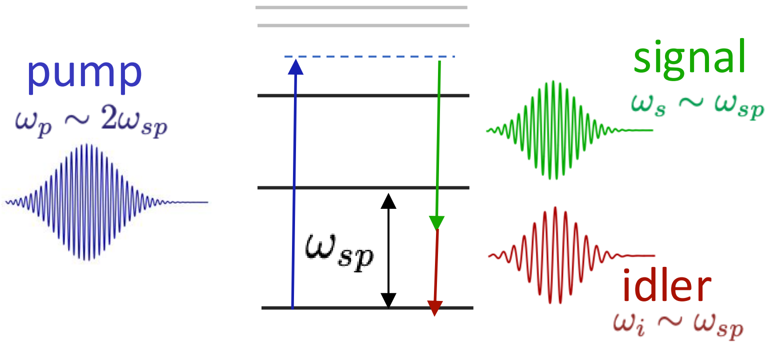

- To start with, we performed a semiclassical estimate of SPDC yield.

SPDC Yield: # of signal/idler photons produced via SPDC per # incident pump photons

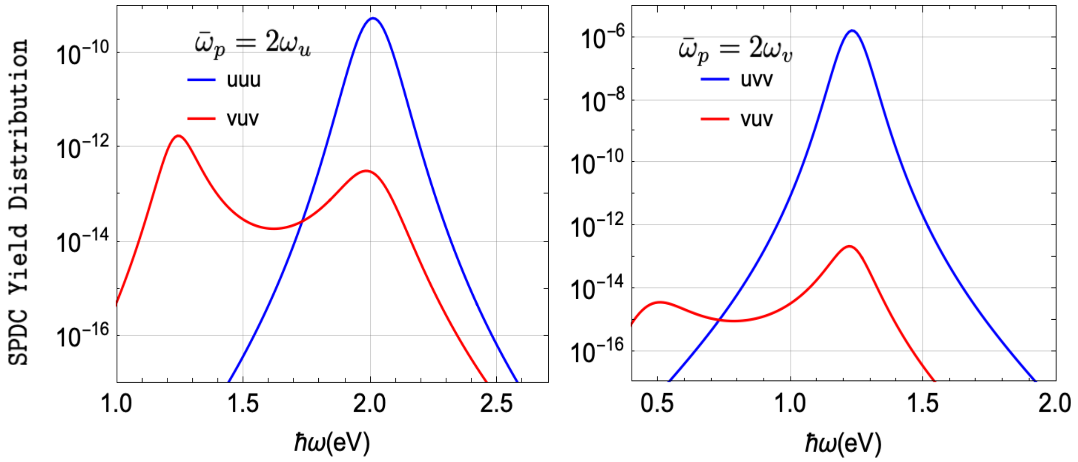

- Yield is enhanced by surface plasmon resonances
- Performance is comparable/exceeding that of 1mm BBO crystal typically used for SPDC processes.

S. A. Shah, M. R. Clark, J. Zyss, M. Sukharev, A. P., (*in preparation*).

Comparison of calculated/measured frequency entanglement entropy for BBO crystal & L-shaped Au-nanoparticle array

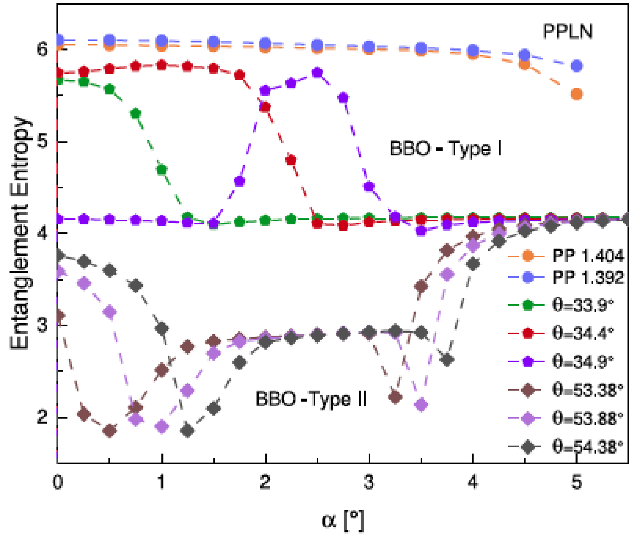

FIG. 4. Entropy calculated on SPDC maps with the gradual variation of angle α from 0° to 5° with 0.25° steps. Different configurations of PM are considered: collinear geometry in PPLN with two different poling periods (PP), non-collinear Type I in BBO crystals and, non-Collinear Type II in BBO crystals with different θ angles.

Our calculations of entanglement entropy for Au-MNP array

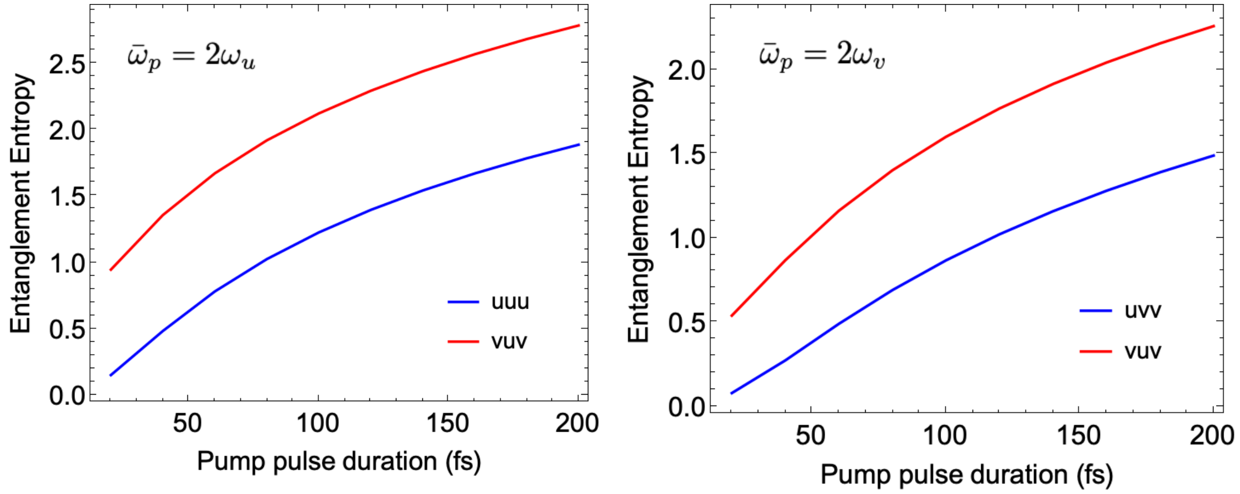

- Entanglement entropy extracted from the experimentally measured JSA for the BBO crystal was reported to be much lower, S=0.78 (Type I) and S=0.78 (Type II).

L. Moretti, et. al., J. Chem. Phys. 159, 084301 (2023)

- Comparing with the calculations for Au MNPs at pulse duration 200 fs (used in the experiment), the MNP produces entanglement entropy $S \sim 2$ which is about two/three-fold lower than that calculated for the BBO crustal but exceeds the values obtained via experimental measurements.

S. A. Shah, M. R. Clark, J. Zyss, M. Sukharev, A. P., (*in prep.*).

Summary & Outlook:

- We explored the use of spinel metal-oxide nanoparticles for plasmonic enhancement of spontaneous spontaneous emission rate of PbS/CdS quantum dots. While layered structures demonstrates about 10-fold Purcell enhancement, most of the energy is lost in heat. Calculations show that patch antenna geometry allows to improve the radiative decay rate.
- Our simulations demonstrated that strong coupling regime can be achieved between Ag-nanopillar arrays leading to surface lattice resonance and assemblies of CdSe quantum dots. This results in up to 10^5 enhancement of the SHG and possible to second harmonic lasing. Experimental validation of our predictions are underway by our collaborators.
- Finally, we considered parametric amplification and quantum photon generation via SPDC in arrays of Au nanoparticles with C_{2v} symmetries. While the parametric amplification requires multi-layered structure, single layer demonstrates SPDC performance comparable with standard BBO crystal source of entangled photons. Our calculations need further experimental validations.
- Currently, we are exploring the effect of plasmonic cavities on the exciton state in 2D TMD materials and more generically the polariton polariton processes in vdW-materials constitute our near-term work.

Acknowledgements

Collaborators: Theory & Simulations

Maxim Sukharev
Arizona State University

Joseph Zyss
Ecole Normale Supérieure
Paris Saclay

Syed Shah
Los Alamos National Lab

Michael Clark
Arizona State University

Experimental collaborators

Han Htoon
Center for Integrated
Nanotechnologies
LANL

Jennifer Hollingsworth
Center for Integrated
Nanotechnologies
LANL

Funding: LANL: Los Alamos Directed Research and Development (LDRD) Funds

ASU: Airforce Office of Science

This work was performed, in part, at the Center for Integrated Nanotechnologies, an Office of Science User Facility operated for the U.S. Department of Energy (DOE) Office of Science. Los Alamos National Laboratory, an affirmative action equal opportunity employer, is managed by Triad National Security, LLC for the U.S. Department of Energy's NNSA, under contract 89233218CNA000001.